PHYSICAL REVIEW C, VOLUME 64, 051301(R)

Intruder states in ^{8}Be

E. Caurier,[1] P. Navrátil,[2] W. E. Ormand,[2] and J. P. Vary[3]
[1]*Institut de Recherches Subatomiques, IN2P3-CNRS-Université Louis Pasteur, Batiment 27/1, F-67037 Strasbourg Cedex 2, France*
[2]*Lawrence Livermore National Laboratory, L-414, P. O. Box 808, Livermore, California 94551*
[3]*Department of Physics and Astronomy, Iowa State University, Ames, Iowa 50011*
(Received 11 July 2001; published 4 October 2001)

Low-lying intruder $T=0$ states in ^{8}Be have been posited and challenged. To address this issue, we performed *ab initio* shell model calculations in model spaces consisting of up to $10\hbar\Omega$ excitations above the unperturbed ground state with the basis state dimensions reaching 1.87×10^8. To gain predictive power we derive and use effective interactions from realistic nucleon-nucleon (NN) potentials in a way that guarantees convergence to the exact solution with increasing model space. Our $0\hbar\Omega$ dominated states show good stability when the model space size increases. At the same time, we observe a rapid drop in excitation energy of the $2\hbar\Omega$ dominated $T=0$ states. In the $10\hbar\Omega$ space the intruder 0^+0 state falls below 18 MeV of excitation and, also, below the lowest 0^+1 state. Our extrapolations suggest that this state may stabilize around 12 MeV. We hypothesize that these states might be the broad resonance intruder states needed in R-matrix analysis of $\alpha-\alpha$ elastic scattering. In addition, we present our predictions for the $A=8$ binding energies with the CD-Bonn NN potential.

DOI: 10.1103/PhysRevC.64.051301 PACS number(s): 21.60.Cs, 21.10.Dr, 21.30.Fe, 27.20.+n

In the R-matrix analysis of $\alpha+\alpha$ elastic scattering and the analysis of ^{9}Be$(p,d)^8$Be and the β decay of ^{8}Li and ^{8}B, very broad 0^+ and 2^+ intruder states at about 10 MeV were inferred [1]. Such states would complement the well-known ground-state rotational band and the 2^+ states at 16.6 and 16.9 MeV, but have not been directly observed. In a separate R-matrix analysis, Warburton did not dispute the need for the inclusion of intruder states, but tried to adjust the interaction radius so that the intruder states appear above 26 MeV of excitation energy of ^{8}Be [2]. Recently, the existence of the low-lying intruder states in ^{8}Be was disputed in multi-$\hbar\Omega$ shell model (SM) and deformed oscillator model calculations [3]. This theoretical work was followed by a Comment [4] and a Reply to the comment [5]. Recently, Barker reevaluated the earlier R-matrix analyses [6] and reemphasized the need for these low-lying intruder states. At the same time, he pointed out that the attempts to fit data without these low-lying intruder states in Ref. [2] led to inconsistent values of R-matrix parameters.

Here, we present results of multi-$\hbar\Omega$ shell model calculations that differ significantly from those in Ref. [3]. First, we extend the basis spaces up to $10\hbar\Omega$. Second, instead of phenomenological interactions, we employ two-body effective interactions derived from realistic NN potentials. We apply the *ab initio* no-core shell model (NCSM) [7,8], with the effective interactions derived in a way that guarantees convergence to the exact solution with increasing model space size.

In the NCSM, we start from the intrinsic two-body Hamiltonian for the A-nucleon system $H_A=T_{rel}+\mathcal{V}$, where T_{rel} is the relative kinetic energy and $\mathcal{V}$ is the sum of two-body nuclear and Coulomb interactions. Since we solve the many-body problem in a finite harmonic-oscillator (HO) basis space, it is necessary that we derive a model-space dependent effective Hamiltonian. For this purpose, we perform a unitary transformation [7–12] of the Hamiltonian, which accommodates the short-range correlations. In general, the transformed Hamiltonian is an A-body operator. Our simplest, yet nontrivial, approximation is to develop a two-particle cluster effective Hamiltonian, while the next improvement is to include three-particle clusters, and so on. The effective interaction is then obtained from the decoupling condition between the model space and the excluded space for the two-nucleon transformed Hamiltonian. The resulting two-body effective Hamiltonian depends on the nucleon number A, the HO frequency Ω, and $N_{\max}$, the maximum many-body HO excitation energy defining the model space. It follows that the effective interaction approaches the starting bare interaction for $N_{\max}\to\infty$. Our effective interaction is translationally invariant. A significant consequence of this fact is the exact factorization of our wave functions into a product of a $0\hbar\Omega$ c.m. component times an internal component. This is another feature that distinguishes our approach from most phenomenological SM studies that involve multiple HO shells.

Our most significant approximation here is the use of the two-body cluster approximation to the effective many-body Hamiltonian. Our method is not variational so higher-order terms may contribute with either sign to total binding. Hence, evaluating the dependence on the basis-space parameters and comparisons with other methods where available help calibrate our convergence.

Once the effective interaction is derived, we diagonalize the effective Hamiltonian in a Slater determinant HO basis that spans a complete $N_{\max}\hbar\Omega$ space. This is a highly nontrivial problem due to very large dimensions we encounter. In the present work we performed the many-body calculation with two completely independent shell model codes. First, we used a newly developed version of the code ANTOINE [13]. Second, we employed the many-fermion dynamics (MFD) shell-model code [14] used in the previous NCSM investigations. Both codes work in the m scheme for basis spaces comprising many major shells and use the Lanczos diagonalization algorithm. The ANTOINE code allows a so-

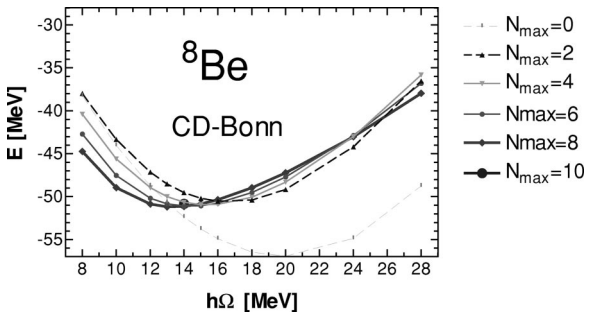

FIG. 1. Ground-state energy of ^{8}Be, in MeV, dependence on the HO frequency for the $0\hbar\Omega$–$10\hbar\Omega$ model spaces using the CD-Bonn *NN* potential. The $10\hbar\Omega$ calculation was performed only at $\hbar\Omega=14$ MeV.

TABLE I. The NCSM results in the $8\hbar\Omega$ basis space for the ground-state energies, in MeV, of ^{8}Be, ^{8}Li, ^{8}B, and ^{8}He using the AV8′ and the CD-Bonn *NN* potentials with Coulomb included. The GFMC results for the AV8′ [16] are shown for comparison. The uncertainties in the CD-Bonn results are deduced from the differences between the NCSM and the GFMC results for the AV8′ *NN* potential. We note the NCSM is not a variational calculation. Thus, more binding does not necessarily imply a better result.

	$AV8'_{GFMC}$	$AV8'_{NCSM}$	$CD\text{-}Bonn_{NCSM}$	Exp
^{8}Be	−47.89(11)	−49.72	−51.18(1.83)	−56.500
^{8}Li	−34.23(14)	−34.84	−35.97(61)	−41.277
^{8}B		−31.39	−32.35(61)	−37.738
^{8}He	−23.76(11)	−24.92	−25.74(1.16)	−31.408

phisticated selection of the pivot vector first by diagonalizing $\hat{J}^2$ in a small model space and second by using the eigenvectors from smaller model spaces as pivots for the larger model spaces. This reduces the number of Lanczos iterations needed for the convergence of the lowest states. Also, the algorithm for the calculation of the Hamiltonian matrix elements is very efficient due to a special basis ordering that allows a very fast generation of all the nonzero matrix elements, which are obtained with just three integer additions. The MFD code, on the other hand, is parallelized using MPI and runs efficiently on parallel machines. It allows one to compute many Lanczos iterations needed to obtain higher lying states and their properties. Also, the wave functions obtained by the MFD can be further processed by a parallelized code that we developed to obtain, e.g., one- and two-body transition densities.

We performed calculations up to the $6\hbar\Omega$ basis spaces, with dimensions $N_D=2\times10^6$, using both codes and cross checked that the same results were obtained. The calculations in the $8\hbar\Omega$ ($N_D=2\times10^7$) and $10\hbar\Omega$ ($N_D=1.87\times10^8$) were performed only using the ANTOINE code.

We present results that we obtained using the nonlocal CD-Bonn [15] *NN* potential and the local Argonne V8′ [16] *NN* potential, which is an isospin invariant, slightly truncated, version of the AV18 *NN* potential. The use of the AV8′ is advantageous since exact solutions were obtained for this potential with the Green's function Monte Carlo (GFMC) method [16].

As our method depends on the basis space size and the HO frequency, we first performed investigations of the ground states of the $A=8$ isobars, ^{8}Be, ^{8}Li, ^{8}B, and ^{8}He in basis spaces from $0\hbar\Omega$ to $8\hbar\Omega$ and for the HO frequency range $\hbar\Omega=8-28$ MeV. In general, we obtain a better convergence rate and a weaker HO frequency dependence for the CD-Bonn *NN* potential. As an example, in Fig. 1 we present the ^{8}Be ground-state energy dependence on the HO frequency for the CD-Bonn calculation. We seek a region where the ground state is approximately independent of the HO frequency. We find this behavior in the largest model space in the range of $\hbar\Omega=12-15$ MeV and we select $\hbar\Omega=14$ MeV for our detailed investigations of the excited states. Also, due to its magnitude, the $10\hbar\Omega$ calculation was performed only for this selected HO frequency. We will publish further details elsewhere.

In Table I, we present the ground-state energies. The NCSM results correspond to the $8\hbar\Omega$ basis space at the minimum of the HO frequency dependence. The binding energies that we obtain with the AV8′ with Coulomb are within 2 MeV of the GFMC results. As the NCSM is not a variational method, more binding in NCSM compared to GFMC does not imply a better result. We use the differences between the NCSM and the GFMC results for the AV8′ *NN* potential to estimate the uncertainty in our CD-Bonn predictions. We note that our CD-Bonn binding energies are about 2–3 MeV larger than the corresponding AV8′ GFMC results, which is a trend consistent with results obtained for lighter nuclei. Still, even the CD-Bonn underbinds the $A=8$ isobars. We conclude that a multinucleon interaction is needed to achieve agreement with experiment.

In Table II, we present the excitation energies that we obtained in the $8\hbar\Omega$ and $10\hbar\Omega$ basis spaces using $\hbar\Omega=14$ MeV. We note that the $10\hbar\Omega$ calculation is very complex. Therefore, we obtained, apart from the ground state and the the intruder $T=0$ 0^+ state that interests us the most, only the lowest 2^+, 1^+, 3^+, and 4^+ states to check the stability of the $0\hbar\Omega$ dominated states. Moreover, we computed the additional four lowest 4^+ states including the $T=0$ 4^+ intruder state using the AV8′ *NN* potential. Let us note that in these $10\hbar\Omega$ calculations we obtained the ground-state energy of −48.323 MeV and of −50.847 MeV with the AV8′ and the CD-Bonn, respectively. We observe a reasonable agreement with experiment with a nearly correct level ordering and small differences between the CD-Bonn and the AV8′ results.

A remarkable feature is the appearance of the intruder $2\hbar\Omega$ dominated 0^+0 state below 20 MeV for both *NN* potentials. In the case of CD-Bonn, this intruder is already below the lowest 0^+1 state in the $8\hbar\Omega$ space. Such an intruder state has not been observed directly, but, as noted above, it might be a candidate for a broad resonance intruder state needed in the *R*-matrix fits of the $\alpha+\alpha$ scattering.

To develop an insight for the evolution of the intruder states with the basis change, we systematically searched for these states in the smaller basis spaces, i.e., from $2\hbar\Omega$ to

TABLE II. The NCSM excitation energies, in MeV, of ^{8}Be using the AV8′ and the CD-Bonn *NN* potentials with Coulomb included. We show the results obtained in the $8\hbar\Omega$ and the $10\hbar\Omega$ spaces using $\hbar\Omega=14$ MeV. The intruder state is denoted by an asterisk.

^{8}Be	AV8′ $^{\hbar\Omega=14\ \mathrm{MeV}}_{\mathrm{NCSM}}$		CD-Bonn $^{\hbar\Omega=14\ \mathrm{MeV}}_{\mathrm{NCSM}}$		Exp
	$8\hbar\Omega$	$10\hbar\Omega$	$8\hbar\Omega$	$10\hbar\Omega$	
$E_x(0^+0)$	0	0	0	0	0
$E_x(2^+0)$	3.595	3.482	3.713	3.613	3.04
$E_x(4^+0)$	12.308	11.949	12.746	12.431	11.40
$E_x(2^+1)$	16.449		16.851		16.63 [a]
$E_x(2^+0)$	16.831		17.238		16.92 [a]
$E_x(1^+1)$	17.419	17.088	17.742	17.789	17.64
$E_x(1^+0)$	17.207	16.822	17.932	17.580	18.15
$E_x(0^+0)$*	19.578	17.812	19.658	17.697	
$E_x(3^+1)$	19.399		19.777		19.01
$E_x(3^+0)$	18.990	18.593	19.567	19.391	19.24
$E_x(0^+1)$	19.139		19.961		
$E_x(4^+0)$	21.030	20.659	21.449		19.86
$E_x(0^+2)$	27.610		28.006		27.49

[a] $T=0$ and $T=1$ components strongly mixed.

$6\hbar\Omega$. In Fig. 2, we present the excitation spectra from $0\hbar\Omega$ to $10\hbar\Omega$ obtained using the AV8′ and $\hbar\Omega=14$ MeV. We observe a very good stability of our low-lying states. In fact, all the $0\hbar\Omega$ dominated states exhibit a reasonable convergence pattern. In the high-lying, incomplete part of the spectra, beginning with the 2 and $4\,\hbar\Omega$ spectra we show the intruder 0^+0 and 2^+0 states, respectively. These states exhibit a dramatic drop in excitation energy with increasing basis space size. In Tables III and IV we exhibit properties of states in ^{8}Be for each of the model spaces. In particular, we outline the configuration decompositions for low-lying states

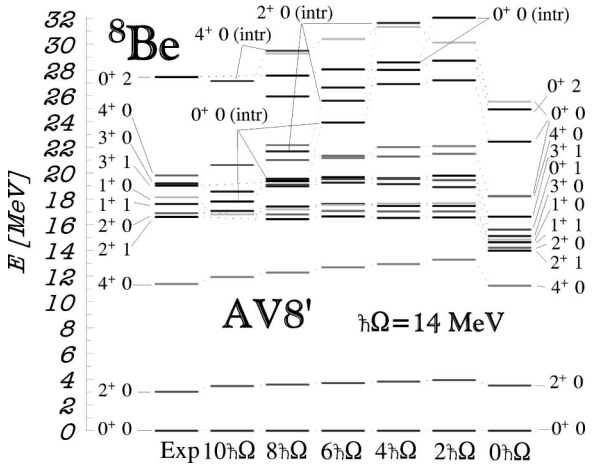

FIG. 2. Experimental and theoretical positive-parity excitation spectra of ^{8}Be. Results obtained in $0\hbar\Omega$–$10\hbar\Omega$ basis spaces using the AV8′ *NN* potential are presented. The HO frequency of $\hbar\Omega=14$ MeV was employed. The experimental values are from Ref. [17]. Above 20 MeV we show only the 0^+ states and the intruder 2^+ and 4^+ states. In the $10\hbar\Omega$ space only the shown states were calculated.

TABLE III. The NCSM excitation energies, in MeV, $B(E2;0_1^+0\rightarrow 2_i^+)$, in e^2 fm^4, and configurations of ^{8}Be 0^+ and 2^+ states as well as the 4^+ intruder state using the AV8′ potential with Coulomb included. Results obtained in the $2\hbar\Omega$ and $4\hbar\Omega$ space using $\hbar\Omega=14$ MeV are presented. Above 20 MeV only selected 2^+ states are shown.

		$2\hbar\Omega$ basis space		
$J^\pi T$	E_x (MeV)	$0\hbar\Omega$	$2\hbar\Omega$	$B(E2\uparrow)$
0^+0	0.0	0.74	0.26	
2^+0	3.940	0.73	0.27	32.513
2^+0	13.308	0.71	0.29	
2^+1	16.588	0.76	0.24	0.057
2^+0	17.054	0.76	0.24	0.040
2^+0	19.392	0.77	0.23	0.084
0^+1	19.482	0.78	0.22	
0^+0	22.132	0.76	0.24	
0^+0	27.226	0.77	0.23	
0^+2	28.756	0.81	0.19	
0^+0	30.160	0.41	0.59	
0^+0	32.088	0.40	0.60	
2^+2	32.872	0.81	0.19	0.003
2^+0	33.678	0.09	0.91	5.742
4^+0	38.901	0.01	0.99	
		$4\hbar\Omega$ basis space		
$J^\pi T$	E_x (MeV)	$0\hbar\Omega$	$2\hbar\Omega$	$4\hbar\Omega$	$B(E2\uparrow)$
0^+0	0.0	0.66	0.20	0.14	
2^+0	3.823	0.65	0.21	0.14	36.397
2^+0	12.947	0.66	0.19	0.15	
2^+1	16.549	0.70	0.16	0.14	0.065
2^+0	17.049	0.70	0.16	0.14	0.069
0^+1	19.571	0.71	0.15	0.14	
2^+0	19.919	0.71	0.16	0.14	0.180
0^+0	22.038	0.68	0.18	0.14	
0^+0	26.936	0.71	0.15	0.14	
0^+2	28.025	0.74	0.12	0.14	
0^+0	28.621	0.13	0.64	0.23	
0^+0	31.387	0.58	0.25	0.16	
2^+0	31.688	0.46	0.36	0.18	2.741
2^+2	32.080	0.74	0.12	0.14	0.068
4^+0	37.941	0.02	0.72	0.26	

and the intruders and the $B(E2;0_1^+0\rightarrow 2_i^+)$ values. Mixing of the $0\hbar\Omega$ dominated states with the intruder states occurs in some model spaces. For example, there are two 0^+0 states in the $2\hbar\Omega$ space with almost identical $2\hbar\Omega$ dominating components. Also, the 0^+0 state at 21.186 MeV in the $6\hbar\Omega$ space has the $0\hbar\Omega$ component under 50% and the 0^+0 state at 23.950 MeV has only 18%. Note the drop in the $8\hbar\Omega$ calculation to a 19.578 MeV intruder state with 20% $0\hbar\Omega$ component. On the other hand, in the $10\hbar\Omega$ basis space, the $0\hbar\Omega$ component of the intruder state at 17.812 MeV is reduced to merely 9%, but the $2\hbar\Omega$ and the $4\hbar\Omega$ components remain at 41% and 21%, respectively. We note that the structure of the intruder states is quite similar in the CD-Bonn calculation.

TABLE IV. The NCSM excitation energies, in MeV, $B(E2;0_1^+0\rightarrow 2_i^+)$, in e^2 fm^4, and configurations of ^{8}Be 0^+, 2^+, and 4^+ states using the AV8′ potential with Coulomb included. Results obtained in the $6\hbar\Omega$, $8\hbar\Omega$, and $10\hbar\Omega$ space using $\hbar\Omega = 14$ MeV are presented. Above 20 MeV only selected 2^+ and 4^+ states are shown. In the $10\hbar\Omega$ space only the shown 0^+ and 2^+ states were calculated.

$6\hbar\Omega$ basis space						
$J^\pi T$	E_x (MeV)	$0\hbar\Omega$	$2\hbar\Omega$	$4\hbar\Omega$	$6\hbar\Omega$	$B(E2\uparrow)$
0^+0	0.0	0.60	0.21	0.12	0.07	
2^+0	3.721	0.59	0.21	0.12	0.08	42.521
4^+0	12.711	0.59	0.21	0.12	0.08	
2^+1	16.655	0.65	0.16	0.11	0.07	0.047
2^+0	17.086	0.65	0.17	0.11	0.07	0.147
0^+1	19.554	0.65	0.16	0.12	0.07	
2^+0	19.926	0.65	0.17	0.11	0.07	0.461
2^+1	20.740	0.66	0.15	0.12	0.07	0.041
0^+0	21.186	0.46	0.30	0.14	0.10	
0^+0	23.950	0.18	0.51	0.18	0.13	
2^+0	25.639	0.39	0.35	0.15	0.11	3.344
2^+0	26.502	0.44	0.31	0.15	0.10	3.819
0^+0	26.679	0.64	0.17	0.12	0.07	
0^+2	28.073	0.70	0.12	0.12	0.06	
0^+0	30.439	0.58	0.21	0.13	0.08	
4^+0	32.652	0.04	0.60	0.21	0.16	
$8\hbar\Omega$ basis space						
$J^\pi T$	E_x (MeV)	$0\hbar\Omega$	$2\hbar\Omega$	$4\hbar\Omega$	$6\hbar\Omega$	$8\hbar\Omega$	$B(E2\uparrow)$
0^+0	0.0	0.57	0.19	0.13	0.06	0.05	
2^+0	3.595	0.56	0.20	0.13	0.06	0.05	48.786
4^+0	12.308	0.55	0.21	0.13	0.06	0.05	
2^+1	16.449	0.63	0.15	0.12	0.05	0.05	0.028
2^+0	16.831	0.62	0.16	0.12	0.05	0.05	0.242
0^+1	19.139	0.60	0.17	0.13	0.06	0.04	
2^+0	19.532	0.60	0.17	0.12	0.06	0.05	1.116
0^+0	19.578	0.21	0.41	0.19	0.12	0.07	
2^+1	20.391	0.63	0.15	0.13	0.05	0.04	0.010
2^+0	21.723	0.46	0.24	0.16	0.08	0.06	4.320
0^+0	22.206	0.40	0.29	0.16	0.09	0.06	
2^+0	23.626	0.24	0.38	0.20	0.11	0.07	6.089
0^+0	25.976	0.58	0.17	0.14	0.06	0.05	
0^+2	27.610	0.66	0.12	0.13	0.05	0.04	
0^+0	29.307	0.43	0.27	0.16	0.08	0.06	
4^+0	29.519	0.09	0.44	0.24	0.15	0.08	
$10\hbar\Omega$ basis space							
$J^\pi T$	E_x (MeV)	$0\hbar\Omega$	$2\hbar\Omega$	$4\hbar\Omega$	$6\hbar\Omega$	$8\hbar\Omega$	$10\hbar\Omega$
0^+0	0.0	0.55	0.19	0.12	0.07	0.04	0.03
2^+0	3.482	0.54	0.19	0.13	0.07	0.04	0.03
4^+0	11.949	0.52	0.20	0.13	0.07	0.04	0.04
0^+0	17.812	0.09	0.41	0.21	0.16	0.08	0.05
4^+0	27.166	0.16	0.32	0.23	0.16	0.08	0.05

Another interesting characteristic of the 0^+0 intruder state is what appears to be a rotational band built on this state. Although the 2^+ states tend to be more mixed because

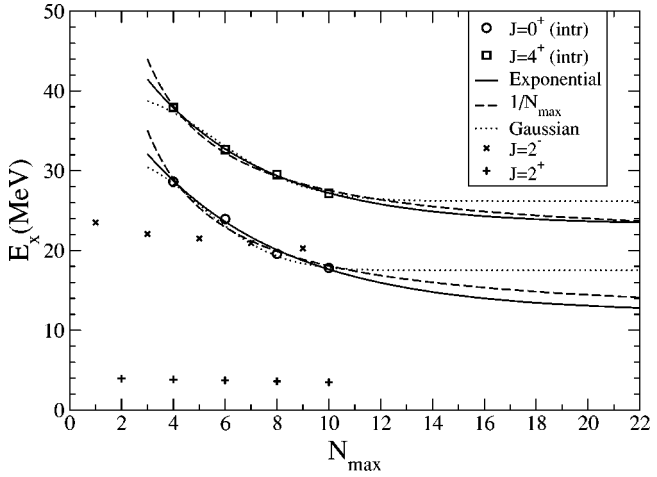

FIG. 3. Plot of the excitation energy of the intruder 0^+ and 4^+ as well as the 2_1^+0 and the 2_1^-0 states as a function of $N_{\max}$. The exponential (solid lines), $1/N_{\max}$ (dashed lines), and Gaussian (dotted lines) extrapolations for the intruders are shown.

of the relatively high density of $0\hbar\Omega$, 2^+ states, the 6 and $8\hbar\Omega$ spaces indicate excitation energies relative to the 0^+ intruder of the order of 3–4 MeV and 9–10 MeV for the 2^+ and 4^+ intruders, respectively. This corresponds to moment of inertia ≈ 1–$1.1\hbar$ MeV^{-1}, which is larger than the value of $\approx 0.88\hbar$ MeV^{-1} as determined from the experimental ground state band.

From the configuration decomposition, in particular in the $10\hbar\Omega$ space, it is quite obvious that the 0^+0 intruder state is not just a simple particle-hole, breathing-mode type, excitation of the ground state. The substantial spreading of the wave function over many higher-$\hbar\Omega$ components suggests a complex structure for the intruder states. This raises interesting questions regarding their physical nature. Four possible explanations come to mind: (1) the states are nonresonant and as $N_{\max}\rightarrow\infty$ will tend to two unbound alpha particles; (2) a beta-type vibration of the ground-state two-alpha cluster; (3) a highly deformed eight-particle cluster, with the excitation energy due to the increased surface energy relative to two alphas; or (4) internal excitation of the alpha particle lowered due to the intercluster interactions. It is first instructive to investigate the convergence of the intruder states. From Tables III and IV it is apparent the rate of decrease in the excitation energy of the intruder states is decreasing, indicating a possible convergence. This is illustrated in Fig. 3 for the AV8′ results for $N_{\max}\geqslant 4$. We can attempt to predict the infinite space result by extrapolating with an exponential dependence in $N_{\max}$, as suggested in Ref. [18], arriving at an excitation energy of 12.2 ± 4.9 MeV for both AV8′ and CD-Bonn. Alternative extrapolation forms, which reproduce the calculated energies equally well, such as $1/N_{\max}$ or a Gaussian, lead to excitation energies of 10.8 ± 1.2 MeV and 17.5 ± 0.3 MeV, respectively. Similarly, we extrapolate the excitation energy for the 4^+ state: 23.2 ± 0.9 (exp), 20.5 ± 0.7 ($1/N_{\max}$), and 26.2 ± 1.1 (Gaussian). The extrapolations are indicated in Fig. 3. In regards to a beta-type vibration, to first order the excitation energy of the 0^+ intruder, 10–17 MeV, is given by the curvature of the restoring force between

the ground-state two-alpha cluster. Given that the ground state is unbound by only 100 keV, such a stiff restoring force is unlikely. On the other hand, a large prolate deformation would require large amplitudes of the higher $\hbar\Omega$ configurations. In any case, the apparent stabilization exhibited for $N_{\max} \geqslant 10$ for the intruder spectrum indicates that the observed 0^+ state is indeed a candidate for the broad resonance required for *R*-matrix analysis of $\alpha-\alpha$ scattering.

As a further check on our calculations, we investigated the negative-parity states using the $1\hbar\Omega-9\hbar\Omega$ basis spaces. In particular, there are experimentally known 2^- and 1^- states at 18.91 MeV and 19.4 MeV, respectively. We obtained the lowest 2^-0 and the 1^-0 states at 20.280 MeV and 21.825 MeV, respectively, in the $9\hbar\Omega$ space relative to the $8\hbar\Omega$ ground state (AV8′,$\hbar\Omega=14$ MeV). Their excitation energy dependence on the basis space resembles more that of the $0\hbar\Omega$-dominated states rather than that of the $2\hbar\Omega$-dominated intruders (Fig. 3). Also, the negative-parity-state $1\hbar\Omega$ dominating component is over 50% in all the spaces we used, contrary to the situation of the intruder states. These findings enhance our confidence in our intruder state results and support our statements about their complexity.

In conclusion, we performed large scale *ab initio* shell model calculations for ^{8}Be using modern *NN* potentials. In the largest basis space that we were able to reach, $10\hbar\Omega$, we observed an intruder 0^+0 state below 18 MeV and below the lowest 0^+1 state with a 2^+0 and a 4^+0 rotational state built on it. Our extrapolation suggests that the 0^+0 intruder state could stabilize at the energy of about 12 MeV. Therefore, we hypothesize that these states are the candidates for the broad resonance intruder states required by the *R*-matrix fits. In addition, we presented our predictions for the binding energies of ^{8}Be, ^{8}Li, ^{8}B, and ^{8}He with the CD-Bonn *NN* potential and compared our Argonne V8′ results with the GFMC calculations.

This was performed in part under the auspices of the U.S. Department of Energy by the University of California, Lawrence Livermore National Laboratory under Contract No. W-7405-Eng-48. P.N. and W.E.O. received support from LDRD Contract No. 00-ERD-028. This work was also supported in part by U.S. DOE Grant No. DE-FG-02-87ER-40371, Division of High Energy and Nuclear Physics.

[1] F.C. Barker, H.J. Hay, and P.B. Treacy, Aust. J. Phys. **21**, 239 (1968); F.C. Barker, *ibid.* **22**, 293 (1969); F.C. Barker, G.M. Crawley, P.S. Miller, and W.F. Steele, *ibid.* **29**, 245 (1976).

[2] E.K. Warburton, Phys. Rev. C **33**, 303 (1986).

[3] M.S. Fayache, E. Moya de Guerra, P. Sarriguren, Y.Y. Sharon, and L. Zamick, Phys. Rev. C **57**, 2351 (1998).

[4] F.C. Barker, Phys. Rev. C **59**, 2956 (1999).

[5] M.S. Fayache, E. Moya de Guerra, P. Sarriguren, Y.Y. Sharon, and L. Zamick, Phys. Rev. C **59**, 2958 (1999).

[6] F.C. Barker, Phys. Rev. C **62**, 044607 (2000).

[7] P. Navrátil and B.R. Barrett, Phys. Rev. C **57**, 562 (1998); **59**, 1906 (1999); P. Navrátil, G.P. Kamuntavičius, and B.R. Barrett, *ibid.* **61**, 044001 (2000).

[8] P. Navrátil, J.P. Vary, and B.R. Barrett, Phys. Rev. Lett. **84**, 5728 (2000); Phys. Rev. C **62**, 054311 (2000).

[9] K. Suzuki and S.Y. Lee, Prog. Theor. Phys. **64**, 2091 (1980); K. Suzuki, *ibid.* **68**, 246 (1982).

[10] J. Da Providencia and C.M. Shakin, Ann. Phys. (N.Y.) **30**, 95 (1964).

[11] E.M. Krenciglowa and T.T.S. Kuo, Nucl. Phys. **A235**, 171 (1974).

[12] K. Suzuki, Prog. Theor. Phys. **68**, 1999 (1982); K. Suzuki and R. Okamoto, *ibid.* **92**, 1045 (1994).

[13] E. Caurier, G. Martinez-Pinedo, F. Nowacki, A. Poves, J. Retamosa, and A.P. Zuker, Phys. Rev. C **59**, 2033 (1999); E. Caurier and F. Nowacki, Acta Phys. Pol. B **30**, 705 (1999).

[14] J.P. Vary, The Many-Fermion-Dynamics Shell-Model Code, Iowa State University, 1992 (unpublished); J.P. Vary and D.C. Zheng, *ibid.*, 1994.

[15] R. Machleidt, F. Sammarruca, and Y. Song, Phys. Rev. C **53**, 1483 (1996).

[16] B.S. Pudliner, V.R. Pandharipande, J. Carlson, S.C. Pieper, and R.B. Wiringa, Phys. Rev. C **56**, 1720 (1997); R.B. Wiringa, Nucl. Phys. **A631**, 70c (1998); R.B. Wiringa, S.C. Pieper, J. Carlson, and V.R. Pandharipande, Phys. Rev. C **62**, 014001 (2000); S.C. Pieper, V.R. Pandharipande, R.B. Wiringa, and J. Carlson, *ibid.* **64**, 014001 (2001).

[17] F. Ajzenberg-Selove, Nucl. Phys. **A490**, 1 (1988).

[18] M. Horoi, A. Volya, and V. Zelevinsky, Phys. Rev. Lett. **82**, 2064 (1999).